JOURNAL OF GEOPHYSICAL RESEARCH, VOL. 86, NO. C2, PAGES 1194–1204, FEBRUARY 20, 1981

Influence of Seasonal Variation Upon the Sensitivity of a Model Climate

RICHARD T. WETHERALD AND SYUKURO MANABE

Geophysical Fluid Dynamics Laboratory/NOAA Princeton University, Princeton, New Jersey 08540

This study investigates the influences of the seasonal variation of solar radiation based upon the results of numerical experiments with a mathematical model of climate. The model consists of (1) a general circulation model of the atmosphere, (2) a heat- and water-balance model of continents, and (3) a simple mixed layer model of the ocean. It has a limited computational domain and idealized geography. Two versions of the model are constructed. In the first version of the model (the seasonal model), a seasonal variation of insolation is imposed at the top of the model atmosphere. On the other hand, an annual mean insolation is prescribed for the second version of the model (the annual model). The response of the seasonal model to the quadrupling of CO_2-concentration in air is compared to the corresponding response of the annual model. It is found that the response of the annual mean surface air temperature of the seasonal model is significantly less than the corresponding response of the annual model. The smaller sensitivity of the seasonal model is attributed to the absence of strongly reflective snow cover (or sea ice) during the summer when the insolation has a near-maximum intensity. A comparison between the hydrologic responses of the seasonal and the annual models indicates that the latitudinal distributions of these responses have qualitatively similar zonal mean features. However, the zonal mean response of the seasonal model is found to have considerable seasonal variations. For example, in summer the zonal mean soil wetness is reduced extensively over two separate zones of middle and high latitudes in response to the CO_2 increase, respectively. Owing to the seasonal variation mentioned above, the latitudinal variation of the annual mean hydrologic response of the seasonal model is less than that of the corresponding response of the annual model.

1. INTRODUCTION

Recently, *Manabe and Stouffer* [1979] investigated the sensitivity of climate to an increase in CO_2 concentration in air with a climate model in which a general circulation model of the atmosphere is coupled with a simple mixed layer model of the ocean. They noted that the sensitivity of their model with seasonally varying insolation is less than the sensitivity of another model with annual mean insolation which was discussed earlier by *Manabe and Wetherald* [1975]. The model of Manabe and Stouffer has a global computational domain and realistic geography, whereas the model of Manabe and Wetherald has a limited computational domain and idealized geography. Therefore, it is not justified to conclude that the aforementioned difference in sensitivity between the two models is attributable to the seasonal variation of insolation. To evaluate the effect of seasonal variation upon the sensitivity of climate, this study compares the sensitivities of two versions of a model with and without seasonal variation of insolation. The basic structure of the model used for this study is very similar to that of the climate model constructed by Manabe and Stouffer. It has, however, a limited computational domain and an idealized geography for the sake of computational economy and ease of interpreting the results of the numerical experiments.

The impact of seasonal variation on the sensitivity of climate is the subject of recent studies by *North and Coakley* [1979], *Thompson and Schneider* [1979], and *Ramanathan et al.* [1979]. These studies investigate the response of zonally averaged energy balance models to either a change in solar radiation or CO_2 content under annual mean and seasonally varying insolation. They noted that the sensitivity of surface air temperature of their models is affected little by the seasonal variation of insolation. Their results differ qualitatively from the results of the present study. This difference is one of the factors which motivated the authors to write this paper.

Paper number 80C1021.

In the previous studies of *Manabe and Wetherald* [1975, 1980] in which they used models with an annual mean insolation, extensive discussions were made not only on the thermal response of a model climate but also on the hydrologic response to an increase of the CO_2 concentration in air. They show that the hydrologic response is far from uniform and has a significant latitudinal variation. This study investigates how this response is altered by the influence of seasonal variation of insolation.

2. MODEL STRUCTURE

The mathematical model of the climate used for this study consists of (1) a general circulation model of the atmosphere, (2) a simple mixed layer model of the ocean with a uniform thickness, and (3) the heat- and water-balance model of continents. The atmospheric model predicts the changes of the vertical component of vorticity, horizontal divergence, temperature, moisture, and surface pressure based upon the equations of the motion, the thermodynamical equation, and the continuity equations of moisture and mass.

The horizontal distributions of the above-mentioned variables are represented by a finite number of spherical harmonics. Fifteen waves are retained in both the zonal and the meridional directions (i.e., higher wave number components are rhomboidally truncated). The model predicts the rates of changes of these variables at all grid points based upon the prognostic equations and transforms them to the spectral domain. This transform method is proposed by *Orsag* [1970] and yields an excellent computational accuracy. The vertical derivatives appearing in the prognostic equations are computed by a finite difference method. The model has nine unevenly spaced finite difference levels in the vertical. The model employs an idealized geography and has a sector computational domain which is bounded by meridians 120° longitude apart and consists of land and mixed layer ocean as Figure 1 illustrates. Cyclic continuity is assumed between these two bound-

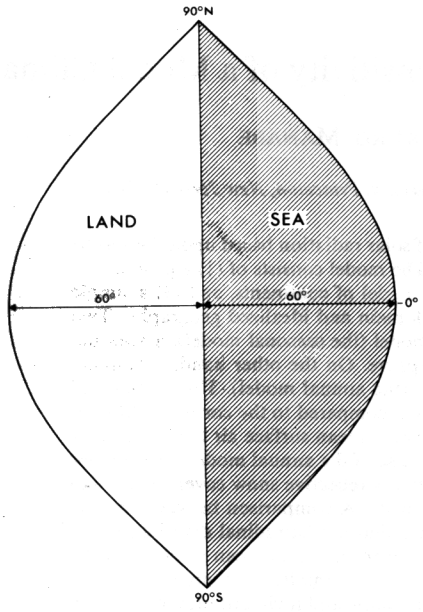

Fig. 1. Computational domain of the model.

aries of meridians. In addition, it is assumed that the earth's surface is flat.

The numerical time integration of the prognostic equations are conducted by a semi-implicit method in which the linear and nonlinear components of the rate of change of a variable are separated and are time integrated implicitly and explicitly, respectively.

The basic structure of the dynamical components of the model described above was developed by *Gordon and Stern* [1974] and is very similar to the spectral model developed by *Bourke* [1974] and *Hoskins and Simmons* [1975]. The readers are referred to these papers for further details.

The distribution of insolation is prescribed at the top of the atmosphere. For the sake of simplicity, the diurnal variation is removed from the insolation. For the computations of both solar and terrestrial radiation fluxes, the effects of clouds, water vapor, carbon dioxide, and ozone are taken into consideration. The mixing ratio of carbon dioxide is assumed to be constant everywhere. A zonally uniform distribution of ozone is specified as a function of latitude, height, and season by use of the data compiled by *Hering and Borden* [1965] and *London* [1962]. Cloud cover is assumed to be zonally uniform and invariant with time based upon the data from the studies of *London* [1957] and *Sasamori and London* [1972]. The distribution of water vapor is determined from the time integration of the prognostic equation of water vapor. Solar radiation is calculated according to a scheme proposed by *Lacis and Hansen* [1974]. Features of the Lacis-Hansen scheme include an improved treatment of Rayleigh scattering and multiple reflections of solar radiation by clouds. Further details of this computation are given in a general circulation study by *Schwarzkopf and Wetherald* [1978]. Terrestrial radiation is computed by the *Rodgers and Walshaw* [1966] method, as modified by *Stone and Manabe* [1968], and includes the *e* type water vapor continuum absorption [*Bignell,* 1970].

Condensation of water vapor is predicted whenever supersaturation is indicated in the computation of the continuity equation of water vapor. Snowfall is predicted when the air temperature near the earth's surface falls below the freezing temperature. Otherwise, rainfall is predicted. The process of moist convection is incorporated through moist convective adjustment. Refer to *Manabe et al.* [1965] for further details of the prognostic system of water vapor.

The temperature of the continental surface is determined such that it satisfies the requirement of heat balance among the net incoming solar radiation, the net outgoing terrestrial radiation, and the fluxes of sensible and latent heat. Over a snow-covered portion of the continent, a high surface albedo of 70% is assumed if the surface temperature is below −10°C, and the albedo of 45% is used if the surface temperature is above this value. Otherwise, a latitudinal distribution of zonal-mean albedo for the bare soil is used [see *Manabe,* 1969, Figure 1*b*]. The change of soil moisture is computed from the rates of rainfall, evaporation, snowmelt, and runoff. A change of the snow depth is predicted as a net contribution from snowfall, sublimation, and snowmelt determined from the heat budget. Refer to *Manabe* [1969] for further details of the hydrologic computations over a continental surface.

The performance of the atmospheric general circulation model described above was examined by *Manabe et al.* [1979*b*]. In particular, they investigated how the quality of the climate simulation is influenced by the spectral resolution of the model. Refer to their paper for further details.

The mixed layer model of the ocean is a vertically isothermal layer of seawater at rest with a horizontally uniform thickness of 68 m. This thickness is chosen to ensure that the heat storage associated with the annual cycle of the observed oceanic temperature is correctly modeled. The rate of the temperature change of the ice-free mixed layer ocean is computed from the heat budget requirement which incorporates the flux of radiation and the exchanges of sensible and latent heat between the ocean and the atmosphere. (The influence of horizontal heat transport by ocean currents and that of heat exchange with the deeper layer of the ocean, however, are not included in this computation.) In the presence of sea ice, the temperature of the underlying water of the mixed layer ocean remains at the freezing point, and the heat flux through the ice is balanced by the latent heat of freezing (or melting) at the bottom of the ice layer. This process, together with the melting at the ice surface, sublimation, and snowfall, determine the change of the ice thickness [*Bryan,* 1969]. For the computation of the net incoming solar radiation, the albedo of sea ice is assumed to be 70% when the surface temperature is below −10°C, and an albedo of 35% is used if the temperature of the sea ice surface is above this value. When the ocean surface

TABLE 1. Length and Number of Seasonal Cycles in Each Stage of the Numerical Time Integrations

Number of Seasonal Cycles	Length of Seasonal Cycle, year	
	Atmosphere	Ocean
	1 × CO_2 Experiment	
5	1/16	1
1	1/8	1
1	1/4	1
1	1/2	1
11	1	1
	4 × CO_2 Experiment	
5	1/16	1
1	1/8	1
1	1/4	1
2	1/2	1
11	1	1

is ice-free, the albedo is prescribed as a function of latitude [see *Manabe*, 1969, Figure 1*b*].

The mixed layer ocean-atmosphere model used here is a modified version of the global climate model, developed by *Manabe and Stouffer* [1979]. Their model has a global computational domain with realistic geography and a slightly different prescription of the surface albedo for snow and ice. Otherwise, these two models are identical. Further details of the mixed layer model will be described in a paper by *Manabe and Stouffer* [1980].

3. PLAN OF NUMERICAL EXPERIMENTS

To investigate the influences of the seasonal variation of insolation upon the sensitivity of the model climate, two versions of the atmosphere-mixed layer ocean model are constructed. The first version of the model is called the 'seasonal model' and has a seasonally varying insolation at the top of the model atmosphere, whereas the second version called the 'annual model' has an annual mean insolation which is invariant with time.

A statistically stationary climate is obtained from a long-term integration of a model. Both the seasonal and annual model are time integrated with a normal (300 ppm) and 4 times the normal (1200 ppm) concentration of carbon dioxide in air. (Hereafter, the time integrations of the model with these two CO_2 concentrations are identified as the ($1 \times CO_2$) and ($4 \times CO_2$) experiment, respectively.) By comparing the difference between the ($4 \times CO_2$) and ($1 \times CO_2$) climates of the seasonal model with the corresponding difference of the annual model, the effect of a seasonal cycle upon the sensitivity of the model climate is evaluated.

The period of time integration, which is required for obtaining a statistically stationary climate of the atmosphere-mixed layer ocean model, is approximately 12–15 years. Since the time integration of the atmospheric part of the model consumes a large amount of computer time and is therefore very costly, an economical method of time integration developed by *Manabe and Bryan* [1969] is used for this study. In short, their method attempts to shorten the length of the atmosphere portion of the time integration required for reaching a statistically stationary model climate. Since the thermal inertia (i.e., heat capacity) of the atmosphere is much smaller than that of the mixed layer ocean, a relatively short-term integration of the atmospheric model is synchronized with the relatively long-term integration of the oceanic model. In the case of the annual model, a 400-day integration of the atmospheric part of the model is synchronized with the 26-year integration of the mixed layer ocean model. This economical integration is followed by a regular 400-day integration of the joint models. In the case of the seasonal model, the time integration of the atmospheric model over an accelerated seasonal cycle is synchronized with a full 1 year (365 days) integration of the mixed layer ocean model. At the beginning of the integration, the period of the accelerated cycle for the atmospheric model is chosen to be 1/16 of a year (i.e., 365/16 ≈ 23 days). It is then increased in several steps by the factor of 2 until this becomes a full year. This economical integration is followed by a regular integration over the period of 11 years. Table 1 tabulates the lengths and the numbers of the atmospheric seasonal cycles for each experiment. It is found that the thermal structures of both the seasonal and the annual models reached the state of statistical equilibrium toward the end of each integration. The results from the annual model, which are discussed in the following sections, represent the time mean state of the model over the last 200-day period of each integration. In the case of the seasonal model, the results from each regular time integration over the last 4-year period are chosen for time averaging and analysis.

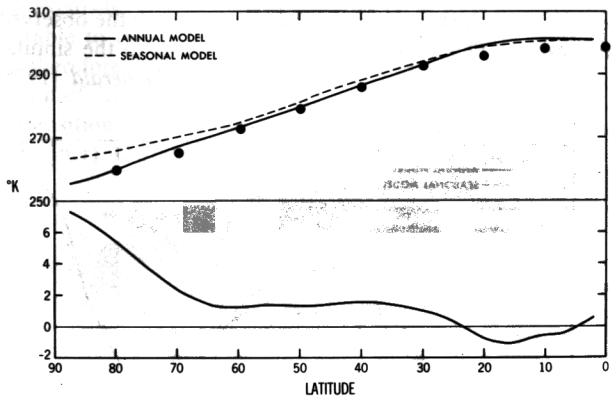

Fig. 2. (Top) Latitudinal distributions of zonal-mean surface air temperature (averages of two hemispheres) for both the annual and seasonal models for the ($1 \times CO_2$) case. Large dots indicate the surface air temperature in the actual atmosphere over the northern hemisphere taken from *Oort and Rasmussen* [1971]. (Bottom) Surface air temperature difference between the seasonal and the annual model for the ($1 \times CO_2$) case. The surface air temperature of the model atmosphere is the temperature at the lowest prognostic level of the model located at the altitude of about 70 m.

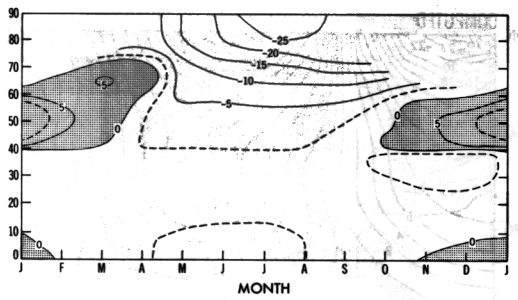

Fig. 3. The latitude-time distribution of the zonal mean difference in the planetary albedo between the seasonal and the annual models. The planetary albedo is defined as the percentage of reflected solar radiation to the incoming solar radiation at the top of the atmosphere. The distributions of the two hemispheres of the model are averaged after shifting the phase of the southern hemisphere variation by 6 months. (Note that the planetary albedo of the annual model is a function of latitude but independent of time.)

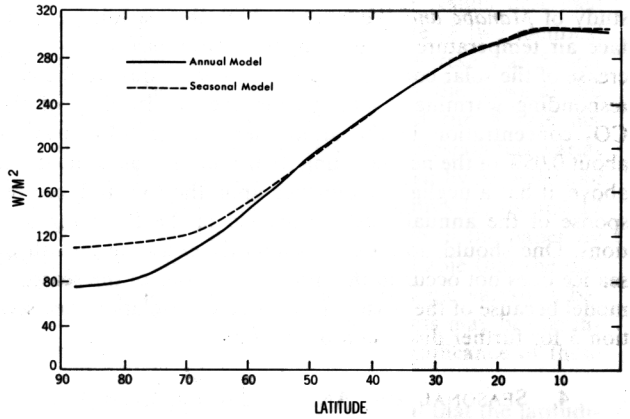

Fig. 4. Latitudinal distributions of net incoming solar radiation (W/m^2) at the top of the seasonal and annual model atmospheres.

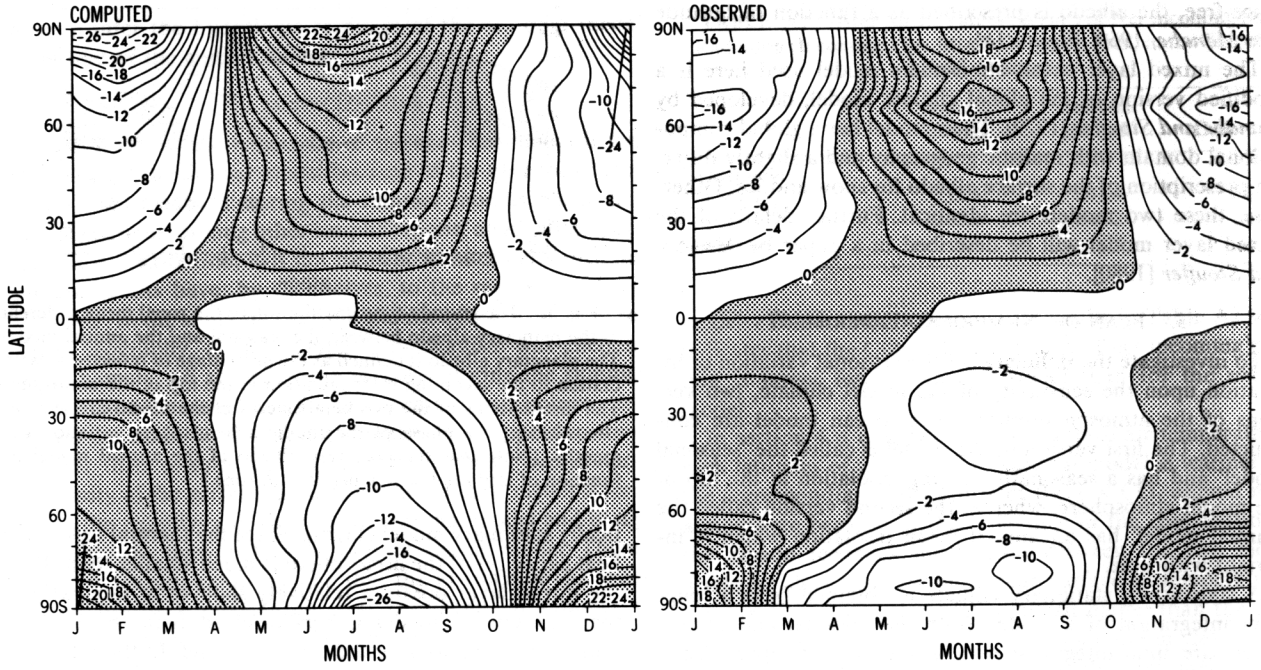

Fig. 5. Latitude-time distributions of the seasonal deviation of the zonal-mean surface air temperature from its annual mean value for the (1 × CO_2) seasonal experiment (left) and actual atmosphere (right). The observed temperature deviations are computed from *Crutcher and Meserve* [1970] for the northern hemisphere and *Taljaard et al.* [1969] for the southern hemisphere. Units are degrees centigrade.

For a further discussion of the economical method of the time integration described above, see the papers by *Manabe and Bryan* [1969] and *Manabe and Stouffer* [1980]. The former discusses the economical integration procedure of an annual model and the latter describes that of a seasonal model.

It is important to note here that the sea ice in high latitudes continues to grow in thickness (but not in the area coverage) throughout the (1 × CO_2) and (4 × CO_2) integrations of the annual model. Obviously, further extensions of the time integrations are necessary to obtain a statistical equilibrium state of sea ice. Averaged over the entire computational domain, the rate of the release of latent heat due to the freezing of sea ice is 0.21 w/m^2 for the (1 × CO_2) experiment and is 0.07 w/m^2 for the (4 × CO_2) experiment toward the end of each integration. Therefore, the difference in these two heating rates is 0.14 w/m^2 which is approximately 0.05% of the net incoming solar radiation at the top of the annual model atmosphere. According to the results from the climate sensitivity study of *Manabe and Wetherald* [1980], the warming of surface air temperature of their model in response to a 4% increase of the solar constant is approximately equal to the corresponding warming resulting from the quadrupling of the CO_2 concentration in the atmosphere. Since 0.14 w/m^2 is about 0.05% of the net incoming solar radiation as pointed out above, it has a negligible influence upon the CO_2-induced response of the annual model discussed in the following sections. One should note that a similarily excessive growth of sea ice does not occur in the time integrations of the seasonal model because of the seasonal variation of insolation. See section 5 for further discussion of this topic.)

4. Seasonal and Annual Model Climates

This section compares the seasonal and the annual model climates with a normal concentration of CO_2. It precedes the following section, which discusses the difference of sensitivity between the two climates.

Thermal Structure

The upper portion of Figure 2 shows the latitudinal distributions of zonal mean surface air temperature from both the seasonal and the annual models together with the corresponding distribution of the actual atmosphere as determined by *Oort and Rasmussen* [1970]. (Here, surface air temperature indicates the temperature at the lowest prognostic level of the model atmosphere which is located at an altitude of about 70 m.) According to this figure, the latitudinal distribution of the zonal mean surface air temperatures of both the seasonal and the annual models compare reasonably well with the observed temperature. This current result is in contrast to the simulation in the earlier study of *Manabe and Wetherald* [1975]

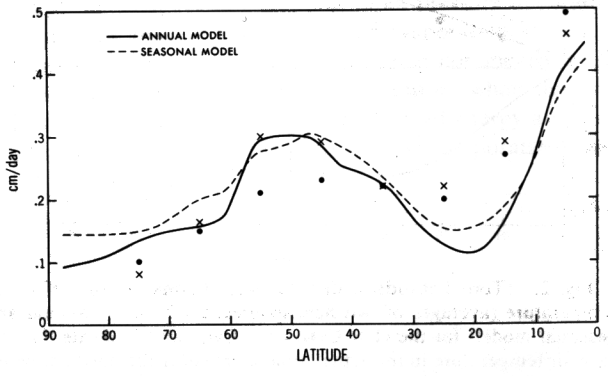

Fig. 6. Latitudinal distributions of zonal-mean total precipitation rate (averages of two hemispheres) for both the annual and seasonal models as well as the observed values for the northern hemisphere (large dots) and southern hemisphere (crosses). Data for the real atmosphere are taken from *Budyko* [1958].

which tended to exaggerate the meridional temperature gradient. It appears that the meridional transport of heat in the spectral atmospheric model adopted for this study is more effective than the transport in the low-resolution grid model which was used by the earlier study.

Figure 2 also indicates that in high latitudes, the zonal mean surface air temperature from the seasonal model is significantly warmer than the corresponding temperature from the annual mode. (Refer to the lower half of Figure 2 which illustrates the temperature difference by a magnified scale.) This difference mainly results from the change in the planetary albedo between the two models, which is illustrated in Figure 3 in a latitude-time representation. This figure indicates that in high latitudes, the planetary albedo of the seasonal model in summer is much less than the time mean planetary albedo of the annual model. This difference results mainly from the disappearance of the highly reflective snow (or sea ice) cover during the summer season when the insolation is relatively intense. On the other hand, the planetary albedo of the seasonal model is more than that of the annual model around 50° latitude in winter. This change is caused by the equatorward extension of the snow (or sea ice) cover during winter when the insolation is relatively weak. These differences in planetary albedo manifest themselves in Figure 4 which shows the latitudinal distributions of zonal mean net incoming radiation at the top of the seasonal and the annual model atmospheres. This figure indicates that in high latitudes, the annually averaged value of net incoming solar radiation at the top of the seasonal model is significantly larger

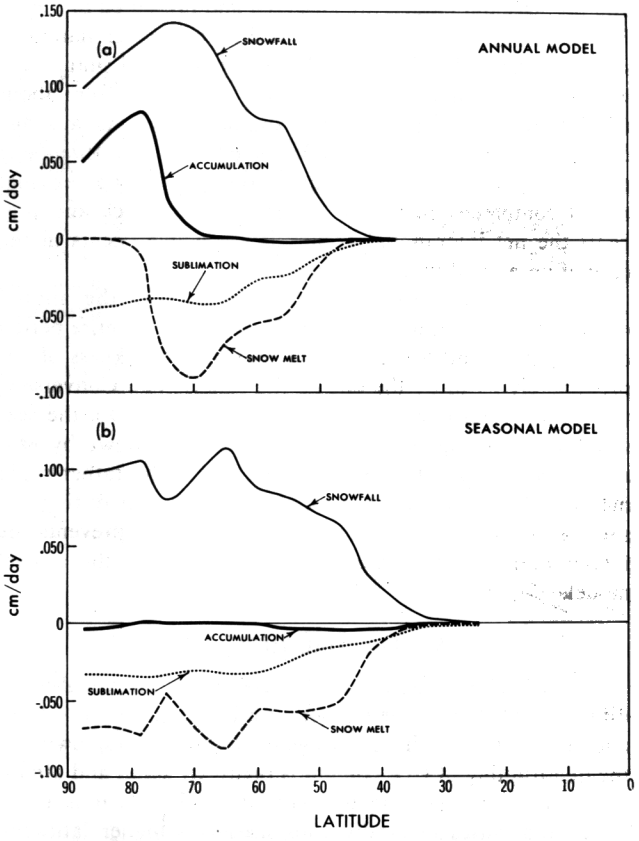

Fig. 7. Zonal mean components of the annual mean snow budget and the zonal mean rate of net snow accumulation over the continent for (*a*) the annual model and (*b*) the seasonal model. The data from the two hemispheres are averaged. Units are in cm/day of water equivalent.

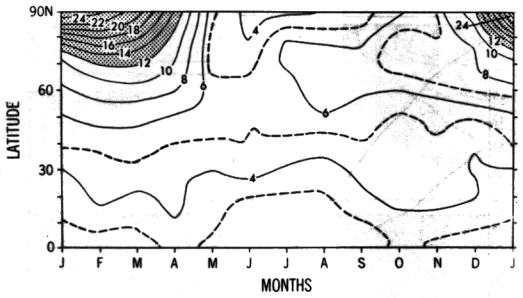

Fig. 8. Latitude-time distribution of the seasonal variation of the zonal mean difference of surface air temperature between the (4 × CO_2) and (1 × CO_2) seasonal experiments. The distributions of the two hemispheres of the model are averaged after shifting the phase of the southern hemisphere variation by 6 months. Units are in degrees Kelvin.

than the corresponding radiation for the annual model, whereas around 50° latitude, the former is slightly less than the latter. In short, the surface air temperature in high latitudes of the seasonal model is higher than that of the annual model mainly because of the absence of the contribution from the albedo feedback mechanism during some of the summer months. Qualitatively similar results were obtained by *Wetherald and Manabe* [1972] in their study of the response of a joint ocean-atmosphere model to a seasonal variation of insolation.

One of the important factors, which determine the difference in the contribution of the albedo feedback mechanism between the seasonal and the annual model, is the amplitude of seasonal variation of the surface air temperature in high latitudes of the seasonal model. Figure 5 compares the simulated distribution of the deviation of the zonal mean surface air temperature from the annual mean values with the distribution of the corresponding variable for the actual atmosphere [*Crutcher and Meserve,* 1970; *Taljaard et al.,* 1969]. This figure indicates that the amplitude of the seasonal variation of surface air temperature around the north pole of the seasonal model is somewhat larger than the observed north polar amplitude, whereas the amplitude at about 70° latitude of the model is smaller than the corresponding observed amplitude. (At lower latitudes, the seasonal model amplitude compares well with the observed.) One should note here that the fractional coverage of the seasonal model ocean is smaller than that of the actual ocean near the north pole and is larger around 70°N. In view of the large thermal inertial of the ocean, it is reasonable that the amplitude of the seasonal temperature variation is exaggerated by the seasonal model at the north pole and is underestimated at about 70°N as described above. One can expect that the exaggeration of the seasonal variation at the north pole and the underestimation at 70°N has an opposing influence upon the area coverage of snow and sea ice during the warm season when insolation is relatively large. The net effect of these discrepancies upon the bias in the sensitivity of the seasonal model has not been evaluated but is probably small.

The observed amplitude over the south pole is much smaller than the polar amplitude of the model. This is due to the large reflection of solar radiation by the Antarctic ice sheet and large thermal inertia of the surrounding ocean.

Hydrology

Figure 6 shows the zonal mean precipitation for the (1 × CO_2) experiment for both the annual and the seasonal models.

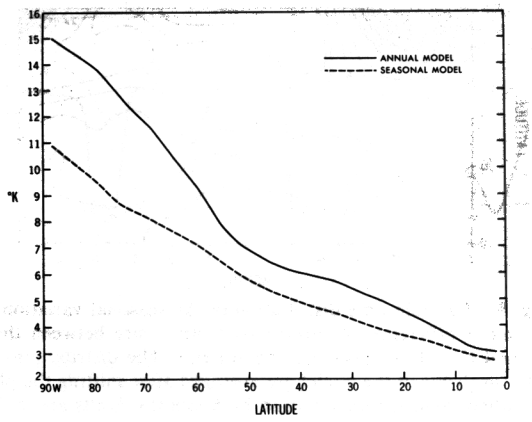

Fig. 9. Latitudinal distribution of the differences in zonal mean surface air temperature (average of two hemispheres) between the (4 × CO_2) and (1 × CO_2) experiments for both the annual and the seasonal models.

In general, the width of both the tropical and the middle latitude rain belts from the seasonal model appear to be wider latitudinally than for those from the annual model. This is due to the seasonal displacement or shift of these two rainbelts with time. Figure 6 also indicates that the tropical rainbelt of the seasonal model appears to be slightly less intense than the annual model. This is, again, due to the seasonal shift of the tropical rainbelt as compared to the constant equatorial position of this rainbelt in the annual simulation.

For the sake of comparison, the observed zonal mean precipitation by *Budyko* [1958] is added to Figure 6 in both the northern and the southern hemisphere, respectively. According to this comparison, the tropical precipitation is systematically underestimated in comparison with the observed distributions. This partly results from the failure of the present model with a relatively coarse resolution to resolve properly the structure of tropical disturbances which yield intense precipitation [*Manabe et al.*, 1979*b*]. It is not clear why the precipitation rates from both the seasonal and the annual models are larger than the observed rates in higher latitudes.

Another important and relevant feature of the hydrologic cycle is the continental snow cover in middle and high latitudes. The annual mean snow budgets from both the annual and the seasonal models are analyzed and presented in Figure 7. According to this figure, there is little net accumulation of snow cover at all latitudes in the seasonal model simulation, whereas there is a net accumulation of snow cover from about 65° latitude to the pole for the annual model. As was discussed by both *Wetherald and Manabe* [1972] and *Manabe et al.* [1979*a*], the intense summer insolation in the seasonal model completely melts the continental snowpack and prevents the net interannual accumulation which occurs in the case of an annual mean insolation.

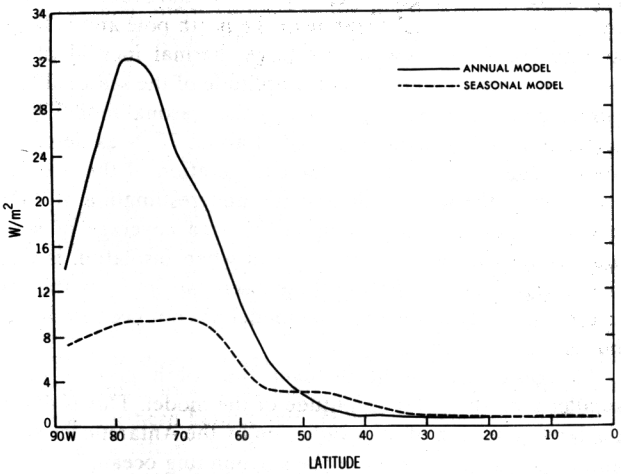

Fig. 10. Latitudinal distributions of the difference in zonal mean net downward solar radiation (average of two hemispheres) at the top of the model atmospheres between the (4 × CO_2) and (1 × CO_2) experiments for both the annual and the seasonal models. The distribution from the seasonal model is an annual mean result.

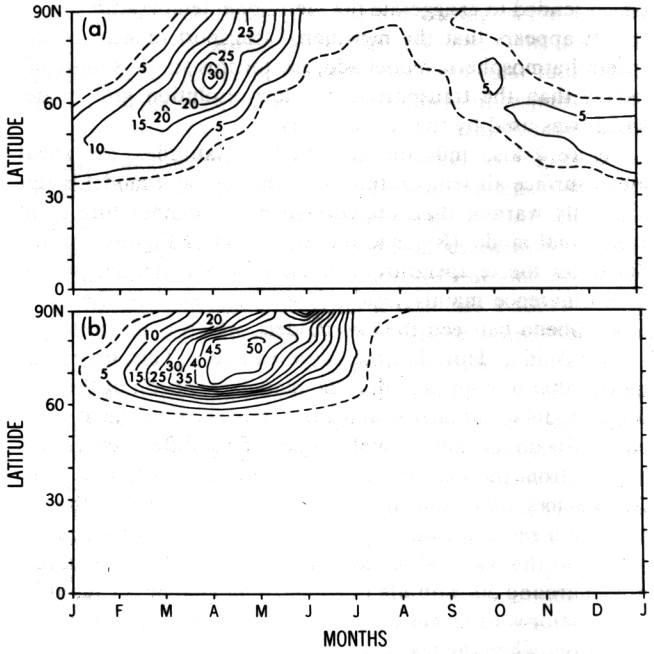

Fig. 11. Latitude-time distributions of the seasonal variation of the zonal mean difference of net downward solar radiation at the top of the model atmosphere between the (4 × CO_2) and (1 × CO_2) experiments over the (*a*) continent and (*b*) ocean. The distributions of the two hemispheres of the model are averaged after shifting the phase of the southern hemisphere variation by 6 months. Units are in W/m².

A similar discussion holds for sea ice. For the annual model, sea ice continued to grow throughout the entire period of integration and had reached a maximum thickness of approximately 25 m by the end of the experiment. Conversely, the average yearly maximum thickness of sea ice for the seasonal model leveled off at about 1 m. As was shown by *Manabe et al.* [1979*a*], this difference is due to the rather rapid melting of sea ice in the seasonal model ocean during the summer season. The intense summer insolation prevents the interannual growth of sea ice which occurs for the annual model.

5. Thermal Response

Figure 8 shows the seasonal variation of the zonal-mean difference of surface air temperature between the (4 × CO_2) and (1 × CO_2) experiments. In general, the warming owing to the quadrupling of CO_2 content is relatively small and almost invariant with season in low latitudes, whereas it is much larger and varies markedly with season in higher latitudes. The large polar warming is at a maximum in winter and is at a minimum in summer. Thus the amplitude of the seasonal variation of surface air temperature decreases from the (1 × CO_2) to the (4 × CO_2) experiment. This result is in qualitative

agreement with the earlier results of *Manabe and Stouffer* [1979, 1980] which were obtained from the global atmosphere mixed layer ocean model with realistic geography. They concluded that the generally strong warming of annual mean surface air temperature in high latitudes results mainly from the poleward retreat of highly reflective sea ice and snow cover. However, the large seasonal asymmetries of the warming were ascribed mainly to the reduction of sea ice thickness which occurs in response to the increase in CO_2 concentration in the model atmosphere. On the basis of the results from their numerical experiments, Manabe and Stouffer concluded that the maximum winter warming in polar latitudes is caused mainly by the increased upward heat conduction through thinner ice. It is encouraging that the present model with an idealized geography yields results which are essentially similar to those obtained from the model with more realistic geography in a global computational domain. (Refer to the study of Manabe and Stouffer for further discussion of this topic.)

Figure 9 shows the latitudinal distributions of the differences in zonal mean surface air temperature between the (4 × CO_2) and (1 × CO_2) experiments. It compares the result from the seasonal model with that from the annual model. According to this figure, the sensitivity of surface air temperature of the seasonal model is significantly less than the annual model. As indicated in Table A1 of the appendix, the area mean value of the CO_2-induced warming from the annual mean model is 6.0°C, whereas the corresponding warming from the seasonal model is 4.8°C. The sensitivity difference between the two models is quite small in low latitudes but becomes pronounced in high latitudes. This suggests the possibility that the effectiveness of the snow (sea ice) albedo feedback mechanism differs between the seasonal and the annual models.

To investigate this possibility, it is decided to analyze the difference in the net downward solar radiation at the top of the model atmosphere between the (4 × CO_2) and (1 × CO_2) experiments. Figure 10 shows the latitudinal distributions of the difference of this quantity from both the annual and the seasonal models. According to this figure, the difference from the seasonal model is significantly less than that from the annual model poleward of 50° latitude. (Refer to Table A2 of the appendix for the area mean values of the differences.) This result implies that the albedo feedback mechanism affects the sensitivity of the seasonal model less than that for the annual model.

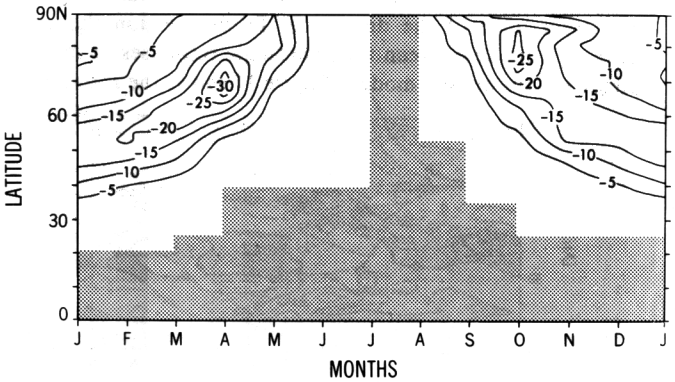

Fig. 12. Latitude-time distributions of the seasonal variation of the zonal mean difference of surface albedo between the (4 × CO_2) and (1 × CO_2) experiments over the continent. The distributions of the two hemispheres of the model are averaged after shifting the phase of the southern hemisphere variation by 6 months. Units are in percent. Shaded region indicates a zero change of surface albedo.

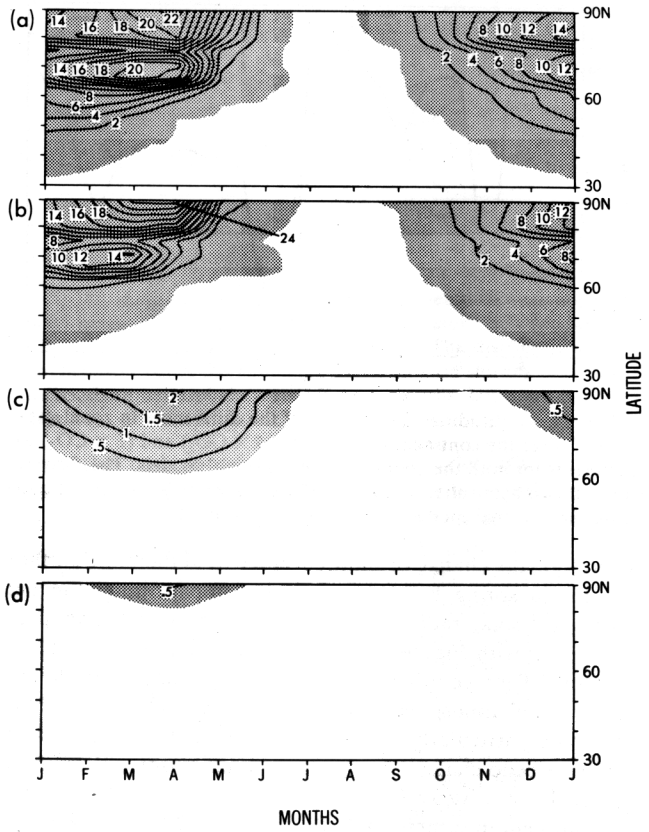

Fig. 13. Latitude-time distributions of the seasonal variation of the zonal mean (*a*) snow depth in centimeter of water equivalent from the (1 × CO_2) experiment (cm), (*b*) snow depth from the (4 × CO_2) experiment, (*c*) ice thickness from the (1 × CO_2) experiment (m), and (*d*) ice thickness from the (4 × CO_2) experiment (m). The distributions of the two hemispheres of the model are averaged after shifting the phase of the southern hemisphere variation by 6 months. Shaded region indicates a change greater than 1 mm for both snow cover and sea ice.

The next step of this analysis deals with the seasonal variation of the difference in the net downward solar radiation at the top of the seasonal model atmosphere between the (4 × CO_2) and the (1 × CO_2) experiments. The latitudinal distributions of zonal mean differences are separated into two parts, namely, the continent (Figure 11*a*) and the ocean (Figure 11*b*). Over the continents there is a distinct belt of large net solar radiation difference starting at around 50° latitude in early spring (March in the northern hemisphere) and progressing poleward until the end of the spring season (May in the northern hemisphere). During summer there is very little difference in the net solar radiation until the fall season (October in the northern hemisphere) where a weak maximum begins to form again and gradually progresses southward as the winter season approaches. The differences in solar radiation, particularly the strong maximum in the spring season, are due to the poleward recession of the highly reflective snow cover from the (1 × CO_2) to the (4 × CO_2) case. Figure 12 which shows the latitude time distribution of the zonal mean difference in surface albedo over the continents, indicates two distinct maximums of comparable magnitudes during both the fall and spring in high latitudes. However, as Figure 11 indicates, the spring maximum of solar radiation difference is much more pronounced than the fall maximum because of the seasonal variation of insolation. In high latitudes the late spring insolation is much larger than the fall insolation.

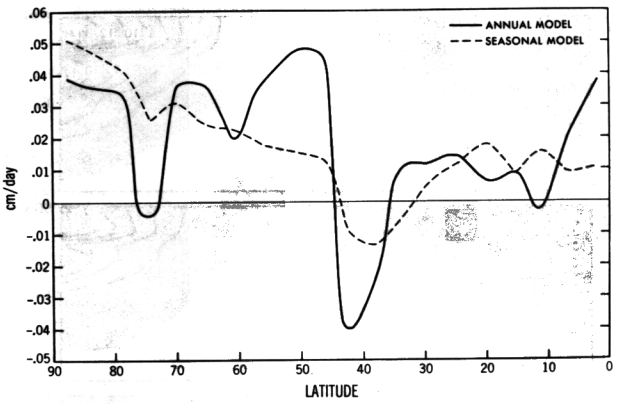

Fig. 14. Latitudinal distribution of the differences in zonal mean ($P - E$) over the continent between the ($4 \times CO_2$) and ($1 \times CO_2$) experiments for both the annual and the seasonal models. The distributions of two hemispheres of the model are averaged. The distribution from the seasonal model is an annual mean result.

Therefore, the change of snow coverage (and therefore surface albedo) in spring has a much larger impact upon the net downward solar radiation than the change in fall (compare Figure 11*a* with Figure 12). In this connection it is significant that the difference in net downward solar radiation at the top of the model atmosphere is very small in summer when the insolation is particularly large. This is consistent with the lack of surface albedo change during the summer season indicated in Figure 12. As discussed later, the snow cover is absent over the continent in summer in both the ($1 \times CO_2$) and ($4 \times CO_2$) experiment and is responsible for the absence of the snow albedo feedback process in this season. (Although Figure 11*a* indicates a small difference in the net incoming solar radiation in July and August, the difference does not result from the change in surface albedo. Instead, it results mainly from the change in the absorptivity of the model atmosphere caused by the change in the water vapor content of air.)

A similar type of analysis may be made on Figure 11*b* which shows the corresponding solar radiation difference over the ocean. Here, the maximum difference is delayed for approximately 1 month in comparison with the continent because the seasonal variation of sea ice lags behind that of the continental snow cover. Again, it is important to note that in late summer, the difference in the net downward solar radiation over the ocean almost vanishes, indicating the absence of sea ice, and accordingly, that of the sea ice albedo feedback mechanism.

Figures 13*a*, 13*b*, 13*c*, and 13*d* show the latitude-time distributions of snow depth and sea ice thickness from the seasonal model for both the ($1 \times CO_2$) and ($4 \times CO_2$) experiments. According to this figure the area coverages of both snow and sea ice obtained from the ($4 \times CO_2$) experiment are significantly less extensive than the coverage in the ($1 \times CO_2$) experiment. It is noteworthy that the snow and the sea ice completely disappear during some of the summer months in both experiments. The disappearance of the snow cover in middle summer is similar to what actually happens in the real atmosphere for the northern hemisphere. However, this is not true for the sea ice variation. As discussed already in section 4, the absence of sea ice during the late summer in the model ocean is probably due to the exaggeration of the amplitude of the seasonal surface temperature variation in the polar region by the present model with an idealized geography (see Figure 5).

The analysis described above indicates that the albedo feedback mechanism does not operate during some summer months when the insolation is relatively large. This is why the annual mean change in the net downward solar radiation at the top of the seasonal model atmosphere in response to the quadrupling of CO_2 concentration is significantly less than the change obtained from the annual model as Figure 10 indicates. Accordingly, it is reasonable that the sensitivity of the seasonal model is significantly less than that of the annual model in which the albedo feedback mechanism operates without interruption over both the continent and the ocean.

From the previous discussion it becomes evident that the mechanism, which is responsible for the sensitivity difference between the two models, is also responsible for making the seasonal model atmosphere warmer than the annual model atmosphere in high latitudes (see section 4). As one can expect, the warmer the surface temperature is, the smaller is the area covered by snow or sea ice and accordingly, the smaller is the influence of the albedo feedback processes. Thus the absence of snow (or sea ice) covered area in summer accounts for not only the relatively high surface temperature in high latitudes but also the relatively low sensitivity of the seasonal model.

In the study of *North and Coakley* [1979], the seasonal fluctuation of continental snow cover is limited considerably owing to the assumption of a zonally uniform permanent ice cap whose boundary position is invariant with season. This assumption restricts the latitudinal range of variable continental snow cover to a zone equatorward of the permanent ice cap boundary. In the studies by *Thompson and Schneider* [1979] and *Ramanathan et al.* [1979], their models do not discriminate the temperature of the continental surface from that of the oceanic surface. Instead, they simulate the latitudinal distribution of zonal mean temperature by introducing the concept of a weighted mean heat capacity of the atmosphere-mixed layer ocean system. Therefore, it is not possible to incorporate properly the effect of the large seasonal variation of continental snow cover into their models. Thus the contribution of the albedo feedback process is substantial in summer as well as other seasons. In view of these factors, it is reasonable that the sensitivities of the seasonal versions of these three energy balance models are almost identical to the sensitivities of their corresponding annual models in disagreement with the present result.

6. HYDROLOGIC RESPONSE

So far, the sensitivity of surface air temperature has been the main topic of the discussion. In this section the comparison is made between the hydrologic responses of the seasonal and the annual models. Figure 14 shows the zonal mean

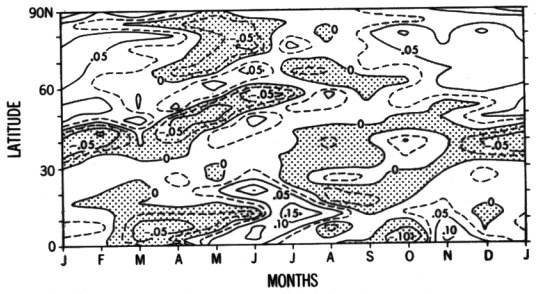

Fig. 15. Latitude-time distributions of the seasonal variation of the zonal mean difference of ($P - E$) between the ($1 \times CO_2$) and ($4 \times CO_2$) experiments with the seasonal model. The distributions in two hemispheres of the model are averaged as indicated by the caption of Figure 13.

difference of $(P - E)$ (i.e., precipitation minus evaporation rate) between the $(4 \times CO_2)$ and $(1 \times CO_2)$ experiments over the continent from both the seasonal and the annual models. In evaluating this figure, it is important to recognize that the annual mean $(P - E)$ is equal to the annual mean rate of runoff in the absence of an interannual change in soil moisture and snow cover. In general, the same qualitative features are evident in both distributions. They are a slight increase of $(P - E)$ in the tropics and subtropics; a rather narrow zone of decreased $(P - E)$, that is, a reduced runoff in middle latitudes; and an increased $(P - E)$, that is, increased runoff in higher latitudes. Similar features were found and were discussed in a study with an annual mean model [*Manabe and Wetherald*, 1980]. In particular, the increased runoff in the tropics and the subtropics occurs mostly along the eastern third of the continent owing to an increased moisture transport along the periphery of the ocean subtropical anticyclone, whereas the zone of reduced runoff in middle latitude is mainly caused by a poleward shift of the middle latitude rainbelt. The increased runoff in higher latitudes is simply a manifestation of an increased poleward transport of moisture from the tropical and subtropical ocean in response to an increase in CO_2 content in the model atmosphere. For further discussion of these characteristics, see *Manabe and Wetherald* [1980].

However, there is an interesting difference between the hydrologic responses of the annual and the seasonal models. In particular, the reduction of $(P - E)$ at around 40° latitude is considerably less for the seasonal model as compared with the annual model. At the same time the increase of $(P - E)$ just poleward of this zone for the seasonal model is not as large as the increase for the annual model. This is due to the seasonal excursion of the middle latitude zone of enhanced aridity (or reduced $(P - E)$). To illustrate this seasonal excursion, Figure 15 is presented. This figure shows the latitude-time distribution of the zonal mean difference of $(P - E)$ between the $(4 \times CO_2)$ and $(1 \times CO_2)$ experiments over the continent obtained from the seasonal model. In this figure, one may note the poleward displacement or latitudinal shift of the area of negative $(P - E)$ from approximately 35° to 55° latitude as the seasons progress from winter to summer. Analysis of the time latitude differences of precipitation indicates that the poleward excursion of this zone of negative $(P - E)$ is directly attributable to the poleward shift of the mid-latitude rainbelt and, therefore, reduced precipitation there with season. The position of this area of negative $(P - E)$ is less obvious during the transition period from late summer (August) to late fall (November). Owing to this seasonal excursion, the annually

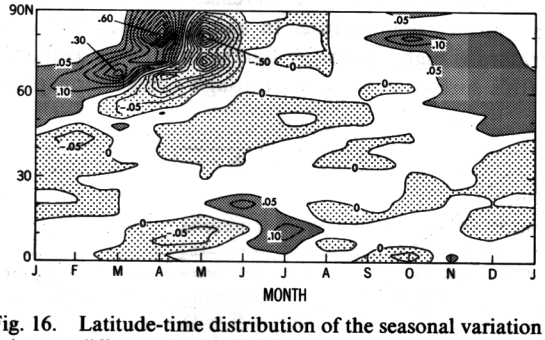

Fig. 16. Latitude-time distribution of the seasonal variation of the zonal mean difference in the runoff rate between the $(1 \times CO_2)$ and $(4 \times CO_2)$ experiments with the seasonal model. The distributions in two hemispheres are averaged as indicated in the caption of Figure 13. Units are in centimeter per day.

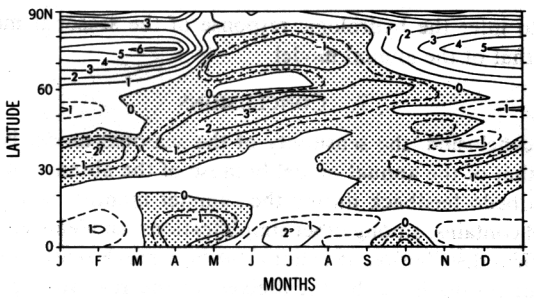

Fig. 17. Latitude-time distribution of the seasonal variation of the zonal mean difference in the soil moisture (cm) between the $(1 \times CO_2)$ and $(4 \times CO_2)$ experiments with seasonal model. Note that the field capacity of soil moisture is assumed to be 15 cm and is constant everywhere. The distributions in two hemispheres of the model are averaged as indicated in the caption of Figure 13.

averaged $(P - E)$ difference around 40° latitude of the seasonal model has a smaller negative value than the corresponding difference from the annual model as pointed out earlier. A qualitatively similar pattern of seasonal excursion is evident in the latitude time distributions of the differences of runoff rate and soil moisture which are shown in Figures 16 and 17, respectively. As one may expect, the negative change of soil moisture follows the spring reduction of $(P - E)$ described above. Thus the CO_2-induced reduction of soil moisture in middle latitude is evident enough through most of the summer season.

In high latitudes the spring snowmelt in the $4 \times CO_2$ experiment occurs approximately 1 month earlier than in the $1 \times CO_2$ experiment owing to the warmer surface air temperature. (This difference of the time of the snowmelt season between the two experiments manifests itself in Figure 16 as two parallel belts of positive and negative differences of the runoff rate.) The earlier snowmelt season in the $4 \times CO_2$ experiment implies a longer duration of the warm period when the soil moisture tends to decrease. Thus in summer the soil moisture in high latitudes from the $4 \times CO_2$ experiment is less than the corresponding soil moisture from the $1 \times CO_2$ experiment. This reduction of soil wetness in high latitudes together with the aforementioned reduction in middle latitudes yields an extensive zone of reduced wetness in summer which is evident in Figure 17. During the remainder of the year (i.e., from fall to spring), the soil wetness in high latitudes increases from the $1 \times CO_2$ to the $4 \times CO_2$ experiment as influenced by the positive $(P - E)$ difference described earlier.

It should be emphasized here that the results described above were obtained from a 4-year average of two identical hemispheres which, when taken together, represent an 8-year average for a single hemisphere. In addition, the seasonal and latitudinal variations of soil moisture and runoff rate described above resemble qualitatively the corresponding variations from the global climate model discussed by *Manabe and Stouffer* [1980]. (For example, compare Figures 15, 16, and 17 from this study with Figures 24, 25, and 26 in the paper by Manabe and Stouffer.) Therefore, it is probable that the differences in the distributions of the hydrologic variables between the $4 \times CO_2$ and $1 \times CO_2$ experiments may be significant even though the tests of statistical significance of these differences have not been made.

The results discussed in this section reveal that the latitudinal distribution of the hydrologic variables varies markedly from one season to another. Therefore, it may not be advis-

able to infer the hydrologic response of the seasonal model from that of the annual model.

7. CONCLUSIONS

In conclusion, the sensitivity of the seasonal model is less than that of the annual model because of the absence of surface albedo feedback during the summer months. Since this model contains, among other simplifications, an idealized geographical distribution, it is not clear how much relevance the present results have, by themselves, to the real atmosphere. However, in the study by *Manabe and Stouffer* [1979], with realistic geography, a similar type of mechanism was encountered, namely, an absence of snow cover during the summer season over the continent for the northern hemisphere. Sea ice, on the other hand, did not completely disappear in summer for their control experiment. The northern hemispheric sensitivity of the surface air temperature of their model is similar to the sensitivity of the present seasonal model and is significantly less than that of the present annual model. Therefore it is reasonable to assume that the absence of the snow albedo feedback mechanism over continents in summer is partly responsible for the relatively small sensitivity of their seasonal model.

A comparison of the hydrologic response of the seasonal and the annual models indicates that many of the zonal mean features of the response found in an annual mean simulation appear to some extent in the seasonal simulation. However, these features, such as the zone of increased aridity in middle latitudes and the zone of increased wetness in higher latitudes are found to undergo considerable seasonal excursions. For example, in summer, the zonal mean soil wetness is reduced extensively over two separate zones of middle and high latitudes respectively in response to the CO_2 increase. Because of the seasonal variation mentioned above, the annually averaged hydrologic response of the seasonal model has a smaller latitudinal variation than the corresponding response of the annual model to the CO_2 increase.

APPENDIX: HEMISPHERIC MEAN TABLES

For more detailed information, the area mean values of two key variables are tabulated in Table A1 and Table A2. They are surface air temperature (i.e., the temperature at the lowest prognostic level located at the altitude of about 70 m) and net incoming solar radiation at the top of the model atmospheres. According to Table A1, the warming of the area mean surface air temperature of the annual model in response to the quadrupling of CO_2 concentration is about 6.0°C and is larger than the corresponding 4.8°C warming of the seasonal model atmosphere. As is discussed in section 5, this difference in sensitivity between the seasonal and the annual model results mainly from the difference in the magnitude of the contributions of the albedo feedback mechanism between the two models. This is underscored by the results in Table A2 which indicates that the CO_2-induced change of net incoming radiation is larger for the annual model than for the seasonal model.

TABLE A1. Area Mean Temperature (°K) of the Model Atmospheres at the Lowest Prognostic Level Located About 70 m Above the Earth's Surface

	Annual Model	Seasonal Model	Difference
Experiment			
$1 \times CO_2$	289.1	289.9	+0.8
$4 \times CO_2$	295.1	294.7	−0.4
Difference	6.0	4.8	

TABLE A2. Area Mean Values (W/m^2) of Net Incoming Solar Radiation (Incoming Flux Minus Outgoing Flux) at the Top of the Model Atmosphere

	Annual Model	Seasonal Model	Difference
Experiment			
$1 \times CO_2$	238.6	241.4	2.8
$4 \times CO_2$	242.8	244.2	1.4
Difference	4.2	2.8	

In section 4 it is shown that the surface air temperature in high latitudes of the $1 \times CO_2$ seasonal model is warmer than the corresponding temperature of the $1 \times CO_2$ annual model atmosphere because of the difference in the contributions of the albedo feedback mechanism between the two models. Table A1 shows that the area mean surface air temperature of the $1 \times CO_2$ seasonal model is indeed higher than the corresponding temperature of the $1 \times CO_2$ annual model by about 0.8°C. Therefore, it is surprising that the area mean surface air temperature of the $4 \times CO_2$ seasonal model turned out to be slightly lower (by 0.4°C) than the corresponding temperature of the $4 \times CO_2$ annual model.

To discuss this result, the latitudinal distribution of the difference in zonal mean surface air temperature between the $4 \times CO_2$ seasonal and $4 \times CO_2$ annual models is shown in Figure A1. (The corresponding result from the $1 \times CO_2$ experiments are also added for the sake of comparison.) According to this figure the surface air temperature in high latitudes of the $4 \times CO_2$ seasonal model is higher than the corresponding temperature of the $4 \times CO_2$ annual model atmosphere. However, the seasonal model temperature is lower than the annual model temperature around 15° and 70° latitudes. A further analysis of the results from the present numerical experiments reveals that this difference in surface air temperature is caused mainly by the enhanced heat removal from the surface owing to the larger rate of evaporation over the continental domain of the seasonal model. Around 15° latitude, this enhanced evaporation occurs because of the increased soil wetness owing to the seasonal excursion of the tropical rainbelt. However, in high latitudes the enhancement occurs because of the large seasonal variation of temperature. Owing to the nonlinear dependence of saturation vapor pressure upon temperature, the relative contribution of evaporation in removing heat from the earth's surface increases nonlinearly with increasing surface temperature. In summer, when the surface temperature is high, the larger fraction of energy available at the earth's surface is removed through evaporation process.

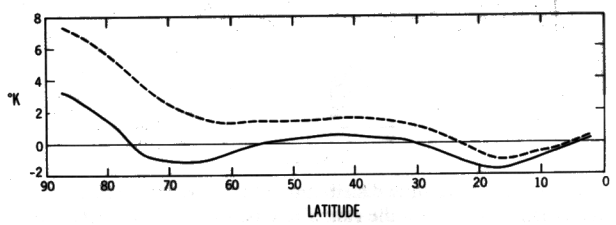

Fig. A1. Latitudinal distributions of the difference in the surface air temperature between the seasonal and annual models. Dashed line: ($1 \times CO_2$) experiments; solid line: ($4 \times CO_2$) experiments.

Thus the annually averaged rate of evaporation from the seasonal model is significantly larger than the rate from the annual model in high latitudes where the amplitude of seasonal temperature variation is relatively large. At the 70° latitude belt, the cooling of the continent surface owing to this effect significantly exceeds the warming owing to the snow cover albedo feedback processes and thus lowers the surface air temperature of the seasonal model atmosphere. A qualitatively similar enhancement of the evaporative cooling owing to the seasonal variation of insolation is evident when one compares the results from the 1 × CO_2 seasonal with those from the 1 × CO_2 annual model. However, the magnitude of the enhancement is smaller around 70° latitude because of the lower surface temperatures of the 1 × CO_2 atmospheres. This smaller enhancement is completely compensated by the warming owing to the snow cover albedo feedback processes for the 1 × CO_2 model atmosphere. This temperature dependence of the evaporative cooling effect in the seasonal model partly accounts for the relatively small sensitivity of the seasonal model when compared with that of the annual model.

Acknowledgments. The authors would like to express their appreciation to L. Holloway, R. Stouffer, and D. Daniel for their large contribution in constructing the computer program of the climate models used for this study. It is a pleasure to acknowledge I. Held and D. Linder who kindly performed a series of numerical experiments similar to the present experiments by use of their energy balance model. The results from their computations were extremely useful for evaluating the results from the present study. Thanks are due to J. Mahlman and S. Fels for their constructive comments on a preliminary version of the manuscript. The authors would also like to thank J. Kennedy, P. Tunison, J. Connor, M. Zadworny, and W. Ellis for prompt and efficient assistance in the preparation of the manuscript.

REFERENCES

Bignell, K. J., The water-vapor infra-red continuum, *Quart. J. Roy. Meteorol. Soc., 96,* 390–403, 1970.

Bourke, W., A multi-level model, 1, Formulation and hemispheric integrations, *Mon. Weather Rev., 102,* 688–701, 1974.

Bryan, K., Climate and the ocean circulation, 3, The ocean model, *Mon. Weather Rev., 97,* 806–827, 1969.

Budyko, M. I., *The Heat Balance of the Earth's Surface,* Office of Climatology, U.S. Weather Bureau, 1958.

Crutcher, H. L., and J. M. Meserve, Selected level heights, temperatures, and dew points for the Northern Hemisphere, *NAVAIR 50-1C-52,* U.S. Naval Weather Ser., Washington, D. C., 1970.

Gordon, T., and B. Stern, The GARP Programme on Numerical Experimentation, *Rep. 7,* World Meteorol. Organ., Geneva, 1974.

Hering, W. S., and T. R. Borden, Jr., Mean distribution of ozone density over North America, 1963–1964, in Environmental Research Papers, *Rep. 162,* U.S. Air Force Cambridge Res. Lab., Hanscom Field, Mass., 1965.

Hoskins, J. J., and A. J. Simmons, A multi-layer spectral model and the semi-implicit method, *Quart. J. Roy. Meteorol. Soc., 104,* 91–102, 1975.

Lacis, A. A., and J. E. Hansen, A parameterization for the absorption of solar radiation in the earth's atmosphere, *J. Atmos. Sci., 31,* 118–133, 1974.

London, J., A study of the atmospheric heat balance, final report, Coll. of Eng., New York Univ., New York, 1957.

London, J., Mesospheric Dynamics, 3, The distribution of total ozone in the Northern Hemisphere, final report, Dep. of Meteorol. and Oceanogr., New York Univ., New York, 1962.

Manabe, S., Climate and the ocean circulation, 1, The atmospheric circulation and the hydrology of the earth's surface. *Mon. Weather Rev., 97,* 739–774, 1969.

Manabe, S., and K. Bryan, Climate calculations with a combined ocean-atmosphere model, *J. Atmos. Sci., 26,* 786–789, 1969.

Manabe, S., and R. J. Stouffer, A CO_2-climate sensitivity study with a mathematical model of the global climate, *Nature, 282,* 491–493, 1979.

Manabe, S., and R. J. Stouffer, Sensitivity of a global climate model to an increase of CO_2-concentration in the atmosphere, in press, *J. Geophys. Res., 85,* 5529–5554, 1980.

Manabe, S., and R. T. Wetherald, The effect of doubling the CO_2-concentration on the climate of a general circulation model, *J. Atmos. Sci., 32,* 3–15, 1975.

Manabe, S., and R. T. Wetherald, On the distribution of climate change resulting from an increase in CO_2-content of the atmosphere, *J. Atmos. Sci., 37,* 99–118, 1980.

Manabe, S., J. Smagorinsky, and R. F. Strickler, Simulated climatology of a general circulation model with a hydrologic cycle. *Mon. Weather Rev., 93,* 769–798, 1965.

Manabe, S., K. Bryan, and M. J. Spelman, A global ocean-atmosphere climate model with seasonal variation for future studies of climate sensitivity, *Dyn. Atmos. Oceans, 3,* 393–426, 1979*a*.

Manabe, S., D. G. Hahn, and J. L. Holloway, Climate simulation with GFDL spectral models of the atmosphere, *GARP Publ. Ser. 22,* World Meteorol. Organ., Geneva, 1979*b*.

North, G. R., and J. A. Coakley, Differences between seasonal and mean annual energy balance model calculations of climate and climate sensitivity, *J. Atmos. Sci., 36,* 1189–1204, 1979.

Oort, A. H., and E. M. Rasmussen, Atmospheric circulation statistics, *NOAA Prof. Pap. 5,* Washington, D. C., 1971.

Orsag, S. A., Transform method for calculation of vector-coupled sums: Application to the spectral form of the vorticity equation, *J. Atmos. Sci., 27,* 890–895, 1970.

Ramanathan, V., M. S. Lian, and R. D. Cess, Increased atmospheric CO_2: Zonal and seasonal estimates of the effect on the radiation energy balance and surface temperature, *J. Geophys. Res., 84,* 4949–4958. 1979.

Rodgers, C. D., and C. D. Walshaw, The computation of infrared cooling rate in planetary atmospheres, *Quart. J. Roy. Meteorol. Soc., 92,* 67–92, 1966.

Sasamori, T., J. London, and D. V. Hoyt, Radiation budget of Southern Hemisphere, in *Meteorology of the Southern Hemisphere, Meteorol. Monogr.,* vol. 13, edited by C. W. Newton, American Meteorological Society, Boston, Mass., 1972.

Schwarzkopf, M. D., and R. T. Wetherald, Sensitivity of a general circulation model to a change in short wave radiation code, paper presented at Third Conference on Atmospheric Radiation of the American Meteorological Society, Davis, California June 1978.

Stone, H. M., and S. Manabe, Comparison among various numerical models designed for computing infrared cooling, *Mon. Weather Rev., 96,* 735–741, 1968.

Suarez, M. J., and I. M. Held, The sensitivity of an energy balance climate model to variations in the orbital parameters, *J. Geophys. Res., 84,* 4825–4836, 1979.

Taljaard, J. J., H. van Loon, H. L. Crutcher, and R. L. Jenne, Climate of the upper air, 1, Southern Hemisphere, vol. 1, in Temperatures, Dew Points and Heights at Selected Pressure Levels, *NAVAIR 50-1C-55,* U.S. Naval Weather Ser., Washington, D. C., 1969.

Thompson, S. L., and S. H. Schneider, A seasonal zonal energy balance climate model with an interactive lower layer, *J. Geophys. Res., 84,* 2401–2414, 1979.

Wetherald, R. T., and S. Manabe, Response of the joint ocean-atmosphere model to the seasonal variation of the solar radiation, *Mon. Weather Rev., 100,* 42–59, 1972.

(Received February 4, 1980;
revised July 21, 1980;
accepted July 22, 1980.)